applied sciences

MDPI

Article

Antibacterial Efficiencies of CVD-PECVD Graphene Nanostructures Synthesized onto Glass and Nickel Substrates against *Escherichia coli* and *Staphylococcus aureus* Bacteria

Elif Orhan [1,*], Betül Aydın [2], Leyla Açık [2], Fatih Oz [3] and Theodoros Varzakas [4,*]

[1] Department of Physics, Gazi University, Ankara 06500, Turkey
[2] Department of Biology, Gazi University, Ankara 06500, Turkey; barslan@gazi.edu.tr (B.A.); leylaacik@gazi.edu.tr (L.A.)
[3] Department of Food Engineering, Atatürk University, Erzurum 25240, Turkey; fatihoz@atauni.edu.tr
[4] Department of Food Science and Technology, University of the Peloponnese, 24100 Kalamata, Greece
* Correspondence: eliforhan@gazi.edu.tr (E.O.); t.varzakas@uop.gr (T.V.)

Featured Application: The antibacterial activities of graphene nanostructures (GrNs) grown onto glass (G) and nickel (Ni) substrates against E. coli and S. aureus have been investigated. The interactions of bacteria with GrNs synthesized onto various substrates (G and Ni) by using different deposition methods (CVD and PECVD) have been examined and the evaluation of these interactions according to the number of layers of graphene and different RF powers has been done. As graphene is transparent, flexible, biocompatible, and thermally stable, the findings may offer new viewpoints both for the better interpreting of the antibacterial activity of GrNs and for the better designing of graphene-based food-packing and biomedical device applications.

Abstract: The antibacterial activity of graphene nanostructures (GrNs) on glass (G) and nickel (Ni) substrates against *Escherichia coli* ATCC 35218 (Gram-negative) and *Staphylococcus aureus* ATCC 25923 (Gram-positive) has been researched in this study. GrNs have been synthesized via two different methods, namely, chemical vapor deposition (CVD) and plasma enhanced chemical vapor deposition (PECVD). While the antibacterial effect of CVD-grown graphene nanosheets has been examined according to the number of layers (monolayer/1–2 layers/2–3 layers), the effect of PECVD grown Gr nanowalls on G substrates has been also analyzed at 100, 150, and 200 W radio frequency (RF) powers. For CVD-grown graphene nanosheets, as the number of layers of graphene nanosheets decreased, the cell viability (%) of *E. coli* decreased from 100% to 51.4%. It has been shown that PECVD graphene nanowalls synthesized onto G substrates, especially at 200 W, exhibited stronger antibacterial activity against *E. coli* and *S. aureus*, and the cell viabilities of *E. coli* and *S. aureus* decreased from 100% to 25.19% and 100% to 9.02%, respectively. It is concluded that that both the nanowall (3D structure) morphology, which changes significantly with the presence of RF power, and the defects created on the graphene surface using the PECVD method are more effective against *E. coli* and *S. aureus* than CVD-grown graphene-based samples (2D-structure).

Keywords: graphene; CVD; PECVD; *E. coli*; *S. aureus*; antibacterial activity

check for updates

Citation: Orhan, E.; Aydın, B.; Açık, L.; Oz, F.; Varzakas, T. Antibacterial Efficiencies of CVD-PECVD Graphene Nanostructures Synthesized onto Glass and Nickel Substrates against *Escherichia coli* and *Staphylococcus aureus* Bacteria. *Appl. Sci.* **2021**, *11*, 7922. https://doi.org/10.3390/app11177922

Academic Editor: Antonio Valero

Received: 6 August 2021
Accepted: 25 August 2021
Published: 27 August 2021

Publisher's Note: MDPI stays neutral with regard to jurisdictional claims in published maps and institutional affiliations.

Copyright: © 2021 by the authors. Licensee MDPI, Basel, Switzerland. This article is an open access article distributed under the terms and conditions of the Creative Commons Attribution (CC BY) license (https://creativecommons.org/licenses/by/4.0/).

1. Introduction

Microorganisms such as bacteria and fungi can easily attach to the surfaces of medical devices and foods and colonize on their surfaces and are a threat to human health and might indirectly lead to economic losses [1,2]. Studies in recent years have shown that some nanomaterials can overcome these threats. Some antibacterial materials, such as metal oxide nanoparticles (NPs) [3], metal NPs [4], and carbon-based nanomaterials (CBNs) [5,6], have been widely studied. Among them, CBNs show amazing traits to combat bacterial infections. Numerous reviews [7–10] on CBNS are available with a different viewpoint and

have been increasing exponentially in the last decade. CBNs such as graphene (Gr) [11], graphene oxide (GO) [11–13], and reduced graphene oxide (rGO) [14] have been established to possess antibacterial activities and have attracted researchers for their antimicrobial properties. Fungi can easily colonize the surfaces of most devices and materials, and they can quickly spread fungal spores. Therefore, suitable material against fungi is extremely desired. The antifungal activities of graphene nanomaterials were studied by synthesizing different types of CBNs, such as Gr, GO, and rGO [2]. The applications of antibacterial and antifungal graphene-based nanomaterials are still relatively novel because a deeper comprehension of the underlying biological mechanisms is required [2].

Gr is a single-atom-thick sheet of hexagonally arrayed sp^2 hybridized carbon atom [15,16]. Gr, obtained for the first time by Novoselov et al. [16], has received great attention from researchers since then because of its electrical and optical properties, as well as its extraordinary physical properties, such as large surface-to-volume ratio, mechanical flexibility, and thermal stability [17–22]. In literature, different methods are used for the synthesis of Gr, such as pulsed laser deposition (PLD), CVD, PECVD, and epitaxial procedures [19–21]. Looking at the practical applications of CVD and PECVD-GrNs, it is seen that GrNs can be synthesized on different substrates. Each procedure depends on many different parameters that play an important role in graphene quality [21,22].

The Gr-based antibacterial tests have been generally applied mainly against *Escherichia coli* (*E. coli*) and *Staphylococcus aureus* (*S. aureus*). As seen in the literature, a lot of researchers have worked on the antibacterial activity of graphene-based materials, especially, Gr, rGO, and GO. Among them, Li et al. [23] showed the antibacterial activity of monolayer Gr films on Cu, Ge, and SiO_2. Especially, the growth of *E. coli* and *S. aureus* were inhibited by graphene films on Cu and Ge. Krishnamoorthy et al. [24] examined the antibacterial activity of Gr nanosheets that could be applied in the development of biomedical devices. They observed that Gr nanosheets have antibacterial activities against *E. coli*. Guihua et al. [25] reviewed the antibacterial and antibiofilm abilities of graphene and its derivatives in solution on the surface. Their toxicity and possible mechanisms were also reviewed. The results showed that the comprehension of the interaction between bacteria and GrNs has critical importance. Dellieu et al. [26] showed that there was no antibacterial activity of CVD graphene films on conductive (Au, Cu) substrates for *E. coli* and *S. aureus*. The conductive substrates do not affect the viability of *E. coli* and *S. aureus* bacteria in contact with CVD graphene films. Kumar et al. [27] wrote the review that summarizes the antibacterial activity of the graphene family and the latest advances that have been made on GrNs, covering the functionalization with metal oxides/ions nanoparticles; silver nanoparticles [28]; and other polymers, enzymes, and antibiotics. Karimi et al. [29] showed the graphene/titanium dioxide nanocomposite-coated cotton specimen to have insignificant toxicity and excellent antimicrobial activity. Akhavan et al. [11] selected *E. coli* and *S. aureus* as model bacteria to investigate the bacterial toxicity of GO and rGO nanowalls. Results showed that bacteria interaction between the very sharp edges of the nanowalls causes cell membrane damage. Again, GO showed the most powerful antibacterial activity under similar concentrations and incubation time among all materials, by graphite, graphite oxide, and rGO [14]. Several studies showed that GO inhibited Gram-positive bacteria more effectively than Gram-negative bacteria, while some Gram-negative bacteria, such as *E. coli*, were resistant to GO [30]. The morphology of the cells plays a vital role in the bactericidal effect of GO. Gram-negative bacteria and Gram-positive bacteria have dissimilar cell wall structures and chemical compositions. The differences observed between Gram-negative bacteria and Gram-positive bacteria could be related to differences in the cell wall structure, cell physiology, metabolism, or degree of contact. Indeed, while peptidoglycan counts for 90% of the cell wall in Gram-positives, it counts only for 5–10% of the cell wall in Gram-negatives. In addition, unlike Gram-positive bacteria, Gram-negative bacteria have an outer lipid membrane [31]. Hu et al. [32] showed that GO and rGO nanosheets significantly inhibited the *E. coli* bacterial growth while showing minimal cytotoxicity. Some researchers [33–35] have studied metal ions/oxides of antimicrobial activities against

bacterial, viral, and fungal pathogens with toxicity against some mammalian cells. Perreault et al. [36] investigated the size-dependency of GO antimicrobial activity using the Gram-negative bacteria *E. coli*. They concluded that smaller sheet sizes can increase the antimicrobial activity of the material. Ibarra-Alonso et al. [37] researched the performance of polyethylene (PE)/clay/silver nanocomposites against *E. coli*. They concluded that the obtained nanocomposites showed enhanced barrier properties and outstanding antimicrobial properties against bacteria, *E. coli*. Pham et al. [38] showed that graphene induces the formation of pores that kill spherical and rod-shaped bacteria. Navorra-Rosales [39] investigated the antibacterial properties of plasma-treated Cu nanoparticles against *P. aeruginosa* and *S. aureus*.

The results showed that the comprehension of the interaction between bacteria and GrNs has critical importance. Hence, the components impacting the interactions and mechanism involved in induced bacterial death should be clarified [27]. The Gr-based antibacterial tests have been generally applied mainly against *E. coli* and *S. aureus.* Looking at the practical applications of CVD and PECVD-GrNs, it is seen that GrNs can be synthesized on different substrates; herein, we have synthesized two kinds of GrNs (graphene nanosheets and graphene nanowalls) onto G substrates. Additionally, monolayer graphene nanosheets have been synthesized onto Ni substrate. To analyze the responses to the GrNs on G and Ni substrates, both Gram-negative *E. coli* and Gram-positive *S. aureus* were used in this study.

In this research, the antibacterial activities of GrNs grown on G and Ni substrates against *E. coli* and *S. aureus* have been investigated. The interactions of bacteria with GrNs synthesized onto various substrates (G and Ni) by using different deposition methods (CVD and PECVD) have been examined and the evaluation of these interactions according to the number of layers of graphene and different RF powers has been done. As graphene is transparent, flexible, biocompatible, and thermally stable, the findings may offer new viewpoints, both for the better interpreting of the antibacterial activity of GrNs and for the better designing of graphene-based food-packing and biomedical device applications.

2. Materials and Methods

2.1. Synthesis and Transfer of Graphene Nanosheets

In this study, Gr nanosheets were produced in two dimensions on Cu foil with 99.99% purity by using the CVD method. Cu foil acts as a catalyst in this process. The foils, which were commercially available from Alfa Easer, were 0.025 mm thick and were cut into 2.5 × 2.5 cm dimensions suitable for the CVD system used for two-dimensional (2D) graphene synthesis. Methane (CH_4), argon (Ar), and hydrogen (H_2) gases were used in all synthesis processes. In the synthesis of 2D graphene, first, using a heater in an H_2 environment, the temperature of the vacuum chamber was raised from room temperature to 1000 °C, then the substrates were annealed at a constant of 1000 °C for 30 min, and finally, methane, argon, and hydrogen gases were used together for graphene synthesis. Gas flow rates of argon, hydrogen, and methane gases were 20 sccm, 30 sccm, and 10 sccm during the graphene synthesis process, respectively. After the synthesis process, the flow of methane and argon gases was cut off, and the temperature of the vacuum chamber was quickly brought to room temperature with the presence of hydrogen gas in the environment. After the 2D graphene synthesis was completed, the transfer of these GrNs onto the G substrates was carried out. Monolayer, 1–2 layers, and 2–3 layers Gr nanosheets were transferred onto G substrates having dimensions of 2.5 cm × 2.5 cm separately by using the polymethyl methacrylate (PMMA) wet transfer method. PMMA was spin-coated on the top of Gr nanosheets, followed by the etching of the Cu foil in aqueous $FeCl_3$ (Transene CE-100). Figure 1 presents the schematic illustration of graphene transfer. The main reason here was to determine the effect of the number of graphene layers on bacterial attachment and bacteria-killing. The synthesis and transfer of Gr nanosheets were explained in detail in our previous studies [19–22]. The procedures for synthesizing Gr nanosheets on Cu foil

are also identical for Ni. Untreated G substrates were also used as negative controls to compare the antibacterial activities of Gr nanosheets synthesized on these substrates.

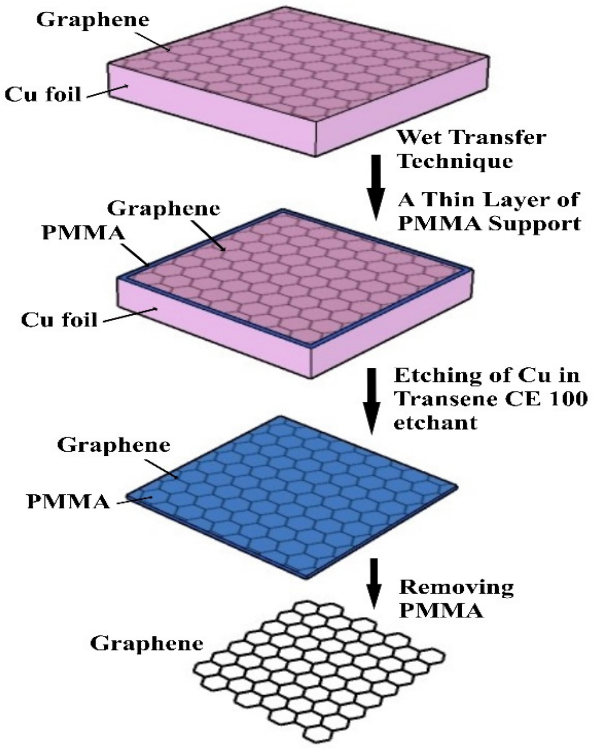


Figure 1. A schematic illustration of graphene transfer.

2.2. Synthesis of Graphene Nanowalls

To research the effect on the antibacterial activity of the PECVD growth mechanism, we also synthesized graphene nanowalls (3D) onto G substrates via the PECVD method at different RF powers. The most important feature that distinguishes this technique from CVD is the RF unit used to produce plasma. First, the G used as substrate was cut in 2.5 × 2.5 cm dimensions and then washed with various chemicals and, finally, rinsed in an ultrasonic bath. After pre-cleaning, G substrates were used for synthesis. In the PECVD technique, Gr nanowalls were synthesized at 100, 150, and 200 W RF powers. In the synthesis process, the temperature of the vacuum chamber was set at 600 °C, and the coating time was 30 min. Ar gas was not used in this technique, and the gas flow rates of other gases were as stated above. The purpose of synthesizing 3D graphene structures, synthesized using the PECVD technique at different RF powers, was to determine the effect of the nanowall morphology, which changes significantly with the presence of RF power, on antibacterial activity. 3D graphene nanowall structure was obtained when the growth temperature of 600 °C was reached. This can be explained by the increase in the concentration and kinetic energy of the carbon-containing radicals at this temperature.

2.3. Characterizations of Synthesized Graphene Nanostructures

In this study, the characterization techniques, such as Raman spectroscopy, scanning electron microscopy (SEM), and transmission electron microscopy (TEM) were employed for the graphene nanostructures.

2.3.1. Raman Analysis

Inelastic scattering of excitation light by the molecules of gaseous, liquid, or solid material is called the Raman effect. The interaction of a molecule with photons gives rise to vibrations of its chemical bonds; this causes a specific energy shift in the scattered light called the Raman spectrum. All chemical samples can be categorized by this individual

spectral fingerprint. A confocal microscope combined with a spectrometer collects Raman spectra. Raman spectroscopy, which is a strong, rapid, sensitive, and non-destructive analytical approach to provide both qualitative and quantitative information for carbon-based materials, is one of the best tools to investigate the structure and quality of carbon-based materials, including Gr. In this study, Raman analyses were performed for the synthesis of GrNs. This characterization was done with WITech alpha 300R at 532 nm laser, and the Raman spectra of GrNs were obtained by the excitation source of 532 nm. D, G, and 2D peaks of graphene, the carbon-based material, were extensively investigated using Raman analysis. Strong G peak and strong D peak indicate good graphitic structure, and 2D-G peak intensity ratio ($I_{2D}/I_G > 2$), on the other hand, confirms monolayer graphene [19–22,40,41]. Raman analysis was preferred for the determination of the number of layers in the present work.

2.3.2. SEM and TEM Analysis

SEM and TEM are usually employed to visualize the morphology and structure of graphene-nanostructures. In this study, SEM analysis was carried out to see the morphology and structure of graphene nanowalls grown by the PECVD method. The surface morphologies of Graphene nanowalls were examined by a Zeiss Sigma 300 model scanning electron microscope operating at 5.00 kV under vacuum. TEM analysis is the most apparent method for determining the number of layers and the wrinkles caused by possible residues in the graphene transfer process, i.e., defects. In this study, TEM analysis was carried out to see the negative effects of the transfer of CVD-grown graphene nanosheets. Samples for the TEM study were prepared by scratching the GNS deposited on Cu foil. All samples were examined by the Hitachi HighTech HT7700 TEM model with a maximum acceleration voltage of 120 kV.

2.4. Antibacterial Activity

E.coli ATCC 35218 and *S. aureus* ATCC 25923 were used to test the antibacterial activities of control groups and materials coated with graphene. All of the coated and uncoated materials were sterilized by using an autoclave at 120 °C for 15 min and placed onto the wells of a 6-well plate.

The bacteria were cultured on a nutrient agar plate at 37 °C for 24 h. The cultured microorganisms were resuspended in a saline solution with a final cell concentration of ~107 cells/mL and transferred on each surface of the sample to a final microbial density of 60 µL/cm^2. Microbial cells transferred to an empty well have been used as control. The plates were then incubated for 3 h at 37 °C. After completion of this incubation cycle, 3 volumes of saline solution were added to each sample. Then, 100 µL of this microbial suspension was spread on the appreciate agar plate and incubated at 37 °C for 24 h. After an incubation period, the colonies were counted. Cell viability was calculated by the following formula: Cell viability (%) = (counts of experimental group/counts of the control group) × 100 (%). All experiments were performed in triplicate and repeated at least twice. The antimicrobial activity of the samples was calculated by comparing the percentage of cell viability of the experimental groups with that of the control samples. Cell viability (inverse to cell death) was monitored to evaluate the antibacterial activity of coated and uncoated samples.

2.5. Statistical Analysis

The data obtained in the present study were subjected to variance analysis. The experiment was set up according to a completely randomized design. The results were analyzed using the SPSS package program (SPSS, 20.0), and Duncan multiple comparison tests were used to evaluating the differences between the average values found. Principal component analysis (PCA) was applied to illustrate the differences between the samples by evaluation of cell viabilities (%) of *E. coli* and *S. aureus.* PCA was conducted by SIMCA 14.1 software.

3. Results

In this study, we have synthesized GrNs via two different methods, namely, CVD and PECVD. The antibacterial effect of CVD Gr nanosheets transferred onto G substrates has been examined according to the number of layers (monolayer/1–2 layers/2–3 layers). The effects of PECVD Gr nanowalls synthesized onto G substrates at 100, 150, and 200 W RF powers have been also analyzed. Furthermore, the antibacterial effect of CVD monolayer graphene nanosheet synthesized onto Ni substrate has been studied. Gram-negative *E. coli* and Gram-positive *S. aureus* were used to examine their response to the GrNs synthesized onto G and Ni substrates. Cell viability (inverse to cell death) was monitored to evaluate the antibacterial activity of coated and uncoated samples.

The characterization process of graphene nanosheets synthesized using the CVD technique was performed by Raman spectroscopy. Raman analyses of monolayer (a), 1–2 layers (b), 2–3 layers (c) Gr nanosheets transferred onto G substrates using the CVD technique are presented in Figure 2a–c respectively. As a result of Raman analysis, it was determined that the Gr nanosheets transferred onto G substrate by the CVD method had a characteristic 2D peak position at 2693 cm^{-1} and a G peak at 1590 cm^{-1}. The number of layers of graphene nanosheets synthesized using the CVD technique was determined by calculating their I_{2D}/I_G ratio. These ratios were calculated as 3.6, 1.98, 0.78, and 0.59, respectively, and thus, it was determined that the thin films were monolayer, 1–2-layer, and 2–3-layers, respectively. These rates determined for monolayer graphene synthesis in our study are well compatible with the literature and our previous studies [19–22]. The I_D peak, which is frequently detected in Raman analysis of carbon-based structures and shows its presence at about 1350 cm^{-1}, was not encountered in these films and confirmed the monolayer graphene structure. TEM analysis was carried out to see the negative effects of the transfer of CVD-grown graphene in Figure 3. TEM image shows that the CVD graph perfectly covered the G used as a substrate, that is, there was no wrinkle, and it was also monolayer.

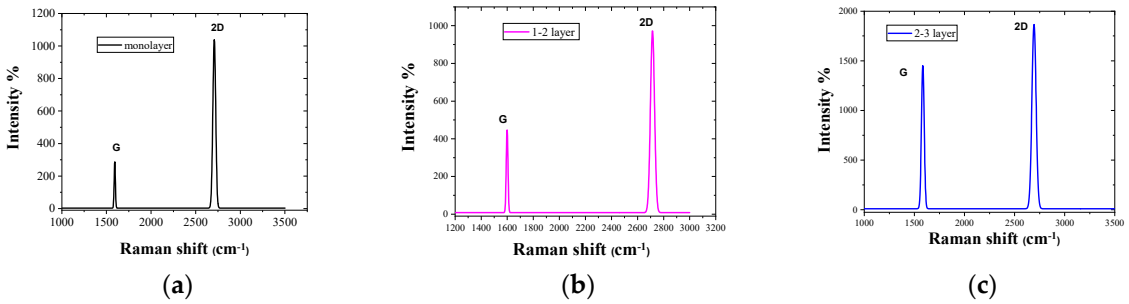


Figure 2. Raman analyses of (**a**) monolayer, (**b**) 1–2 layers, and (**c**) 2–3 layers Gr nanosheets, which were transferred onto G substrates using the CVD technique.

The characterization process of graphene nanowalls synthesized using the CVD technique was also performed by Raman spectroscopy. Raman analysis showed that the Gr nanowalls synthesized on the G substrates with 100, 150, and 200 W RF power by PECVD method had D peaks at approximately 1347 cm^{-1}, G at 1590 cm^{-1}, and 2D peaks at 2690 cm^{-1} [42,43]. The D peaks were quite severe compared to the other peaks, and similarly, the intensity of the 2D peak was quite weak compared to the others. Representation of the D peak was interpreted as defective of the structure and these defects were explained by the presence of a plasma [43]. Similarly, the structural properties of Gr nanowalls synthesized on G substrates at various RF power values (100, 150, and 200 W) using the PECVD technique were examined by Raman analysis and are presented in Figure 4a–c, respectively. Digital photographs of the CVD and PECVD grown graphene samples on G and Ni substrates are given in Figure 5. SEM analysis was carried out for the graphene nanowalls. SEM images at different magnifications for the graphene nanowalls produced at 600 °C were taken and are shown in Figure 6. From SEM images, the homogeneous

structure of PECVD-grown graphene nanowalls and the nanowalls thickness are more clearly seen.

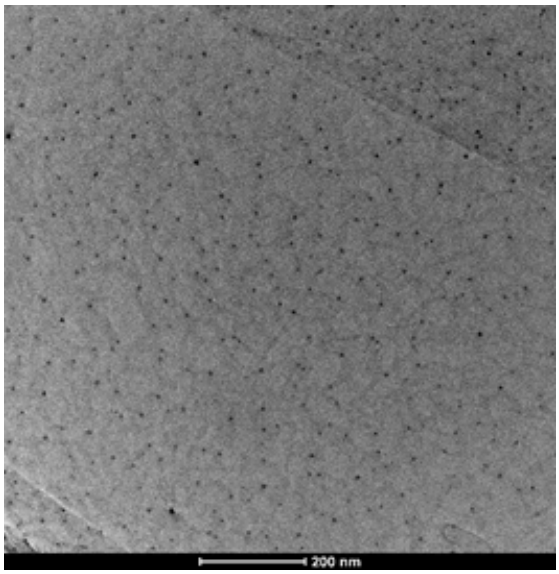
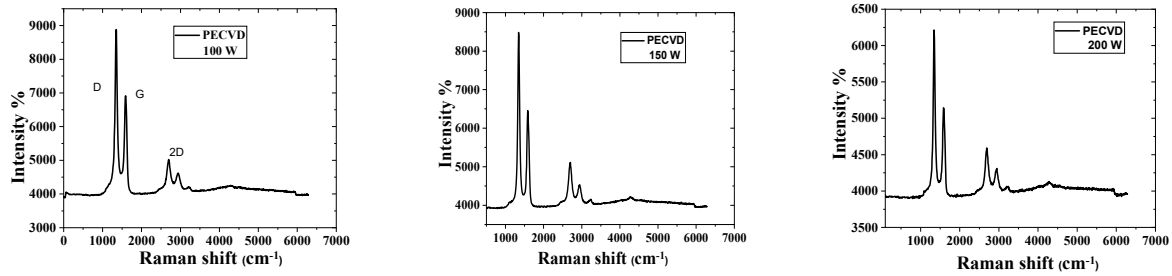
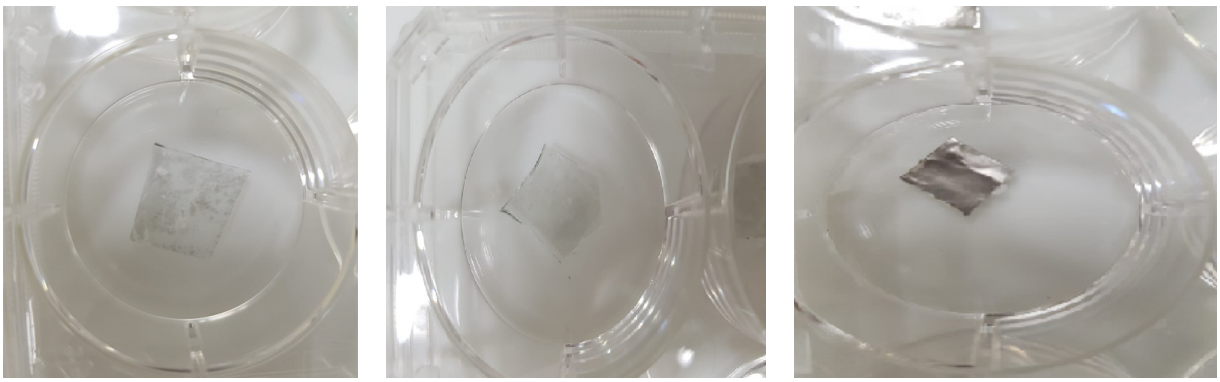


Figure 3. TEM image of CVD grown monolayer graphene.



(**a**) (**b**) (**c**)

Figure 4. Raman analyses of Gr nanowalls synthesized using the PECVD technique at (**a**) 100 W, (**b**) 150 W, (**c**) 200 W.



(**a**) (**b**) (**c**)

Figure 5. Digital photographs of (**a**) PECVD-grown Gr on glass substrate, (**b**) CVD-grown monolayer Gr on glass substrate, (**c**) CVD-grown monolayer Gr on Ni substrate.

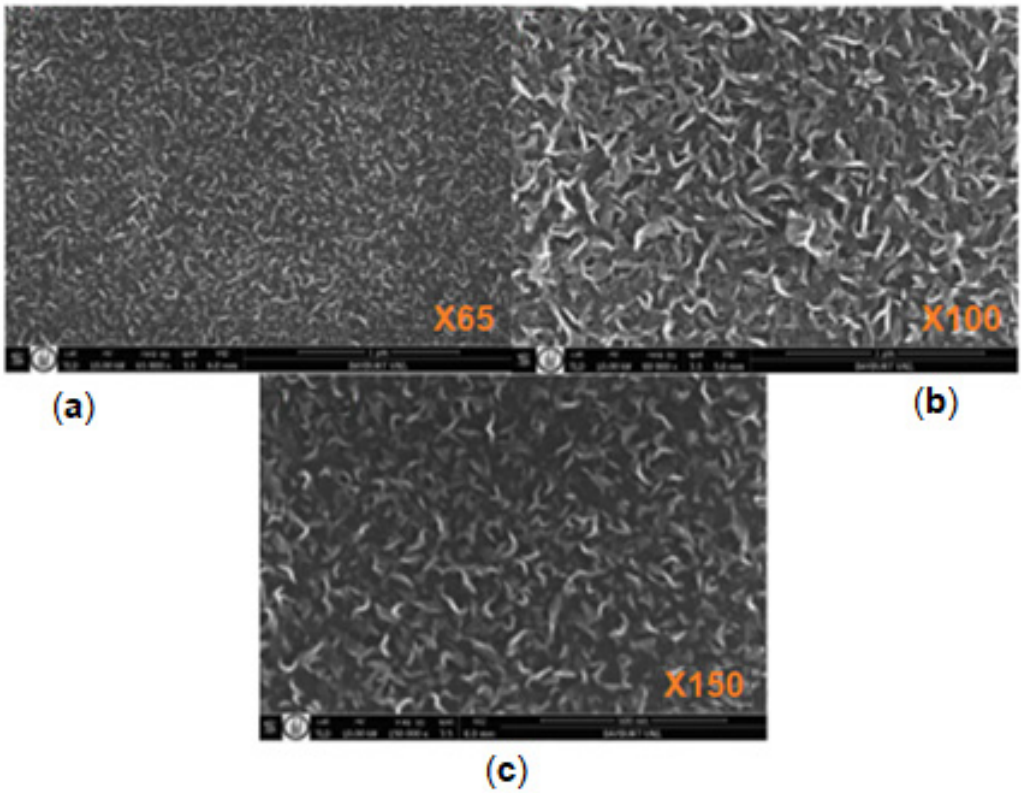


Figure 6. SEM images of PECVD grown graphene nanowalls at different magnifications at (**a**) ×65, (**b**) ×100, and (**c**) ×150.

Figure 7 exhibits the cell viability (%) of *E. coli* and Figure 8 shows the cell viability (%) of *S. aureus*. The antibacterial activities of the samples against *E. coli* and *S. aureus* are shown in Figures 9 and 10, respectively. It is observed that GrNs on the substrates show different antibacterial activities.

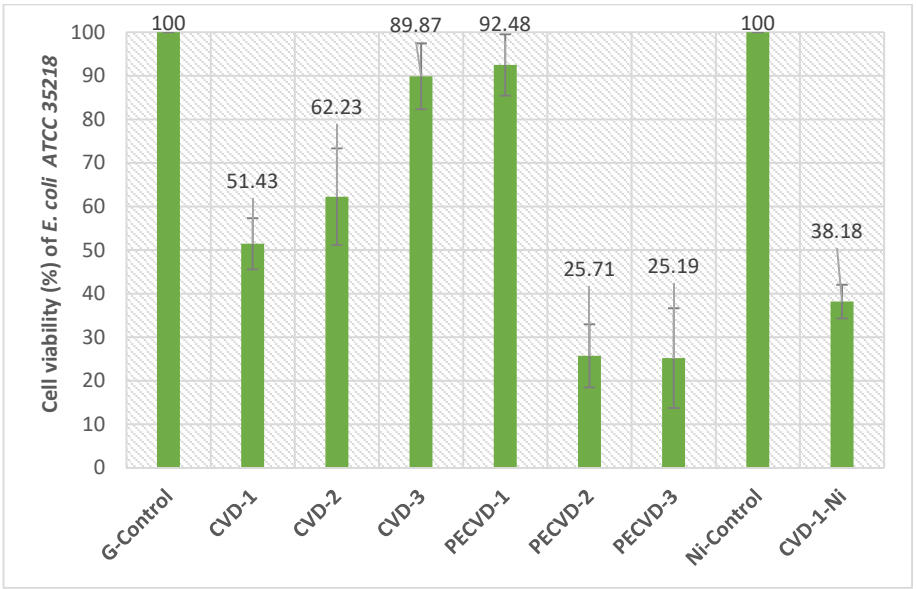


Figure 7. Cell viability (%) of *Escherichia coli* ATCC 35218.

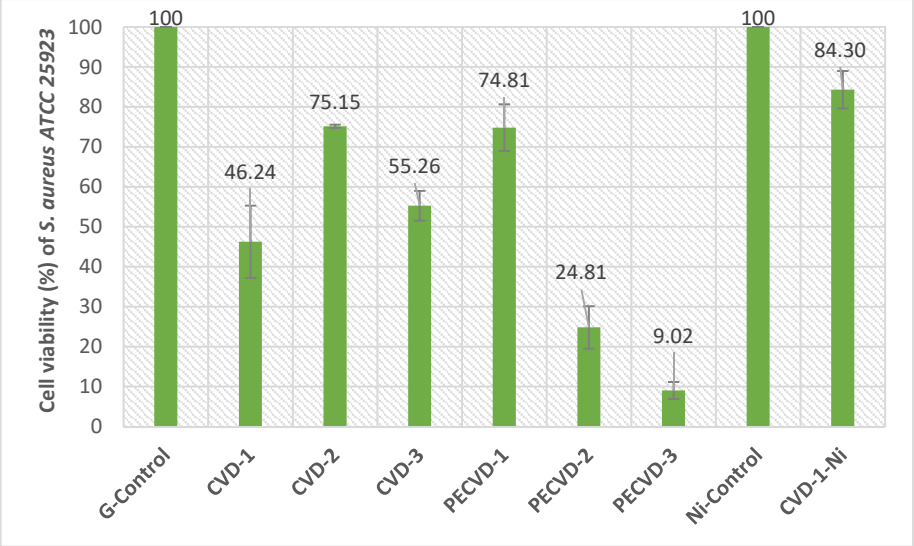


Figure 8. Cell viability (%) of *Staphylococcus aureus* ATCC 25923.

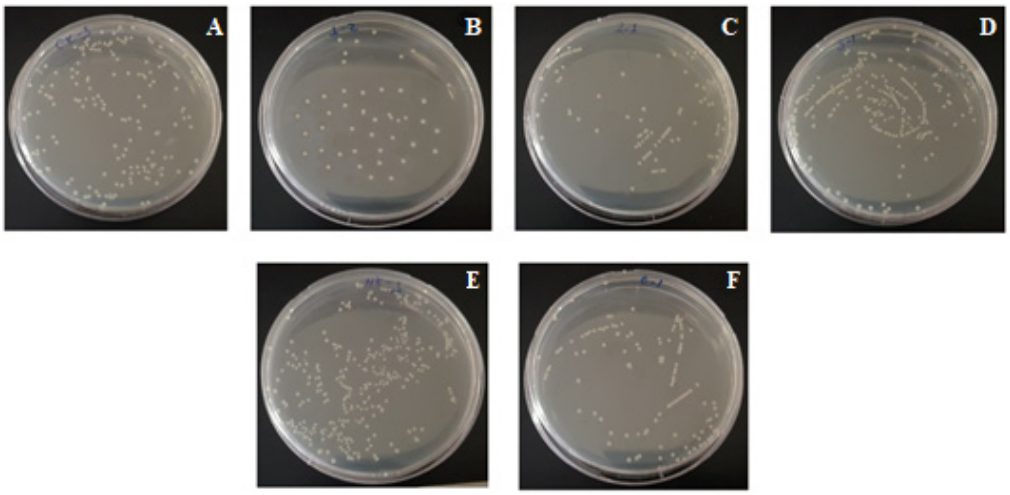


Figure 9. Antibacterial activity of *Escherichia coli* ATCC 35218 ((**A**) glass control; (**B**) CVD-1; (**C**) CVD-2; (**D**) CVD-3; (**E**) Ni Control; (**F**) CVD-1-Ni).

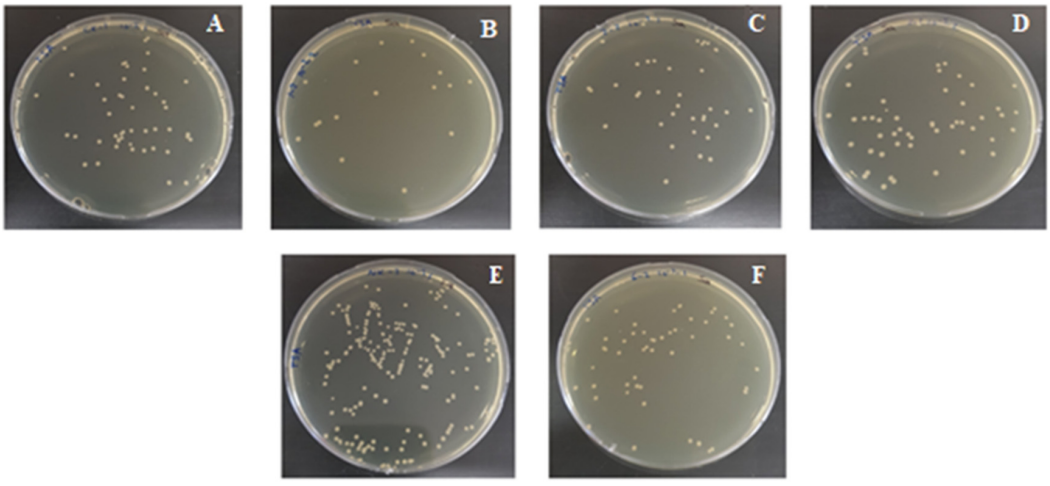
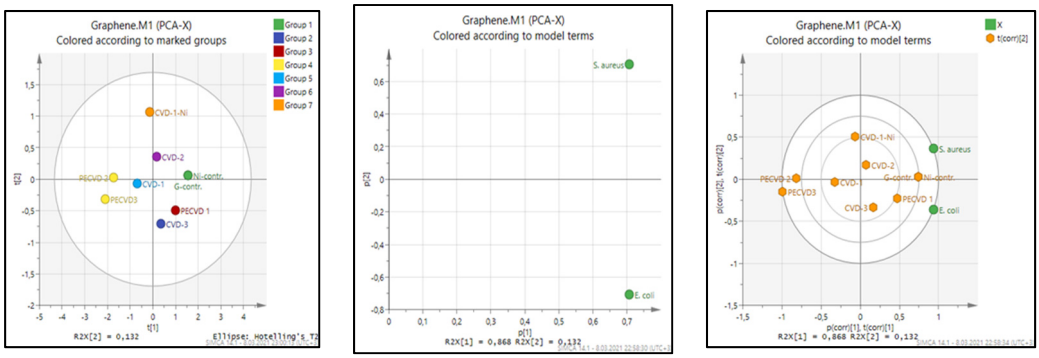


Figure 10. Antibacterial activity of *Staphylococcus aureus* ATCC 25923 ((**A**) glass control; (**B**) CVD-1; (**C**) CVD-2; (**D**) CVD-3; (**E**) Ni Control; (**F**) CVD-1-Ni).

For CVD Gr nanosheets transferred onto G substrates, as the number of layers of GrNs decreased, the cell viability (%) of *E. coli* decreased from 100% to 51.4%. Additionally, the antibacterial effect of CVD monolayer GrN synthesized onto Ni substrate has been studied. In the case of CVD graphene nanosheets synthesized onto Ni substrate, the cell viability (%) of *E. coli* decreased from 100% to 38.18%. It is also concluded that the antibacterial activity against *E. coli* CVD monolayer Gr nanosheets synthesized onto Ni substrate was better than CVD monolayer graphene nanosheets onto G substrate. It has been observed that the antibacterial activity of *S. aureus* was extremely weak (from 100% to 84.3%) for the samples grown on Ni substrate. Li et al. [23] showed the antibacterial activity of monolayer Gr films on Cu, Ge, and SiO_2. In particular, the growth of *E. coli* and *S. aureus* were inhibited by graphene films on Cu and Ge. Krishnamoorthy et al. [24] examined the antibacterial activity of Gr nanosheets that can be applied in the development of biomedical devices. They observed that Gr nanosheets have antibacterial activities against *E. coli*. It is seen that the findings are compatible with the literature.

As can be seen from the experimental results, PECVD Gr nanowalls synthesized onto G substrates, particularly at 200 W, exhibited stronger antibacterial activity against *E. coli* and *S. aureus*, and the cell viabilities of *E. coli* and *S. aureus* decreased from 100% to 25.19% and 100% to 9.02%, respectively.

The data obtained in the present study were also subjected to variance analysis. PCA was applied to illustrate the differences between the samples by evaluation of cell viabilities (%) of *E. coli* and *S. aureus*. The score scatterplot, loading scatter plot, and biplot for the samples are shown in Figure 11a–c, respectively.



(**a**) (**b**) (**c**)

Figure 11. Score scatter plot (**a**), loading scatter plot (**b**), and biplot (**c**) of principal component analysis (PCA) (PC1 versus PC2) for the attributes in the samples.

Using PCA analysis, we examined the experimental results. The first two principal components (PC1 = 86.8% and PC2 = 13.2%) accounted for 100.0% of the variance. PECVD-2 and PECVD-3 were clustered together, and they were well separated from the other samples (Figure 11a), indicating that they had some differences. On the other hand, as can be seen from Figure 11a, no other treatment was included in the same group. Both cell viabilities (%) of *E. coli* and *S. aureus* were positioned at the right side of the plot (Figure 11b,c), while PECVD-2 and PECVD-3 were located at the left part of PC1 (Figure 11c). This result showed that PECVD-2 and PECVD-3 treatments were the treatments where the most inhibition on the cell viabilities (%) of *E. coli* and *S. aureus* was achieved (Figure 11c).

In the current study, it was determined that the graphene treatments had a significant ($p < 0.01$) effect on the cell viability (%) of *E. coli*. The effect of graphene treatments on the cell viability (%) of *E. coli* is shown in Table 1. While the treatments of CVD-3 and PECVD-1 were not statistically different from the control groups (G-control and Ni-control), the highest inhibition on the cell viability (%) of *E. coli* was statistically found in the treatments of PECVD-3, PECVD-2, CVD-1-Ni, and CVD-1.

Table 1. Variance analysis of the effect of graphene treatments on the cell viability (%) of *E. coli* and *S. aureus.*

Treatment	*E. coli*	*S. aureus*
Control	100.00 ± 0.00 a	100.00 ± 0 a
CVD-1 (CVD grown 2D-Monolayer Gr onto glass substrate)	51.00 ± 3	46.50 ± 9 c
CVD-2 (CVD grown 2D-1–2 layers Gr onto glass substrate)	61.50 ± 18	75.00 ± 0 b
CVD-3 (CVD grown 2D-2–3 layers Gr onto glass substrate)	90.00 ± 25 ab	55.50 ± 4 c
PECVD-1 (PECVD grown 3D-Gr-100 W onto glass substrate)	99.50 ± 25 a	75.00 ± 6 b
PECVD-2 (PECVD grown 3D-Gr-150 W onto glass substrate)	28.50 ± 13 c	25.00 ± 6 d
PECVD-3 (PECVD grown 3D-Gr-200 W onto glass substrate)	25.50 ± 9 c	9.50 ± 2 e
CVD-1-Ni (CVD grown 2D-Monolayer Gr onto Ni substrate)	38.00 ± 4 c	84.50 ± 5 b
Sign	**	**

a–e: means with different letters in the same column are significantly different ($p < 0.05$); Sign: Significance; ** $p < 0.01$.

In the current study, it was also determined that the graphene treatments had a significant ($p < 0.01$) effect on the cell viability (%) of *S. aureus*. The effect of graphene treatments on the cell viability (%) of *S. aureus* is also reported in Table 1. As can be seen from Table 1, all treatments caused a significant decrease in the cell viability (%) of *S. aureus*. As well as in *E. coli*, the most inhibition on the cell viability (%) of *S. aureus* was also statistically found in the treatment of PECVD-3.

4. Discussion

In this study, the antibacterial activity of GrNs on G and Ni substrates against *E.coli* (Gram-negative) and *S. aureus* (Gram-positive) was investigated. First, the antibacterial effect of CVD-grown graphene nanosheets on G was examined according to the number of layers (monolayer/1–2 layers/2–3 layers). For CVD-grown graphene nanosheets, as the number of layers of graphene nanosheets decreased, the cell viability (%) of *E. coli* decreased from 100% to 51.4%. It is concluded that monolayer graphene nanosheets have a more antibacterial effect than multilayer graphene (MLGr) nanosheets. Monolayer graphene has different and unique properties compared to MLGr. It is also known that as the number of layers decreases, graphene shows many interesting and different properties.

Furthermore, the antibacterial effect of CVD monolayer graphene nanosheet synthesized onto Ni substrate was studied. In the case of CVD graphene nanosheet synthesized onto Ni substrate, the cell viability (%) of *E. coli* decreased from 100% to 38.18%. It is concluded that the antibacterial activity of CVD monolayer graphene nanosheet synthesized onto Ni substrate against *E. coli* was better than that of CVD grown monolayer graphene nanosheet on G substrate. This result is thought to be due to the fact that the graphene grown on the Ni substrate contains many grain boundaries, and the graphene concentration increases at the grain boundaries [44]. It has been shown also that the cell viability (%) of *S. aureus* was extremely weak (from 100% to 84.3%) for the samples grown on Ni substrate. Therefore, it may be concluded that the monolayer graphene nanosheets grown on the Ni substrate are not effective against Gram-positive *S. aureus*. We conclude that more studies are needed on the effects of transition metal substrates on Gram-positive bacteria.

The antibacterial effect of Gr nanowalls grown on G substrates by the PECVD meth-od was also analyzed at 100, 150, and 200 W radio frequency (RF) powers. It was shown that

PECVD graphene nanowalls synthesized on G substrates, especially at 200 W, exhibited stronger antibacterial activity against *E. coli* and *S. aureus*, and the cell viabilities of *E. coli* and *S. aureus* decreased from 100% to 25.19% and 100% to 9.02%, respectively. Gr nanowall (3D structure) morphology changes significantly with the presence of RF power. Gr nanowalls become more tightly packed with the increase of RF power. Raman spectroscopy revealed that Gr nanowalls were 3D oriented. It was concluded that 200 W RF power had a significant effect onto the tightly packed structure of these vertically oriented (3D) nanostructures.The high antibacterial activity against the two types of bacteria can reflect its potential in food preservation used as a food preservative. It is also concluded that PECVD grown graphene nanowalls on G substrates are more effective against Gram-positive *S. aureus* than Gram-negative *E. coli.*

As a result, it is evident that the antibacterial activities of 3D graphene nanowalls grown on G substrate are stronger than 2D graphene nanosheets grown on G substrate against *E. coli* and *S. aureus*. According to the experimental results, we could also say that the antibacterial activities of PECVD grown graphene samples are more effective against *E. coli* and *S. aureus* than CVD-grown graphene samples. It can also be said that both the nanowall (3D structure) morphology, which changes significantly with the presence of RF power, and the defects created on the graphene surface using the PECVD method are more effective against *E. coli* and *S. aureus* than CVD-grown graphene-based samples (2D-structure). It may also be thought that PECVD grown graphene against *S. aureus* is more effective than against *E. coli*. The differences observed between the viability of the *E. coli* and *S. aureus* could be related to differences in the cell wall structure, cell physiology, metabolism, or degree of contact. Indeed, while peptidoglycan counts for 90% of the cell wall in Gram-positives, it counts only for 5–10% of the cell wall in Gram-negatives. In addition, unlike Gram-positive bacteria, Gram-negative bacteria have an outer lipid membrane [31].

5. Conclusions

It has been shown that PECVD graphene nanowalls synthesized on G substrate, especially at 200 W, exhibited stronger antibacterial activity against *E. coli*. and *S. aureus*. It can also be said that the antibacterial activities of PECVD grown graphene samples are more effective against *E. coli* and *S. aureus* than CVD grown graphene samples. With the increase in RF power, we can expect more tightly packed 3D structures and defects on the graphene surfaces. This may create a better antimicrobial effect. It may also be thought that PECVD grown graphene against *S. aureus* is more effective than against *E.coli*. It is also concluded that the cell viability (%) of *E. coli* CVD monolayer GrNs synthesized onto Ni substrate was better than CVD monolayer GrNs synthesized onto G substrate. It was observed that the cell viability (%) against *S. aureus* was extremely weak for the samples grown on Ni substrate.

As a result, it has been deduced that substrate materials, deposition method, and the number of layers of graphene affect the antibacterial properties of the samples. We have concluded that each sample created from graphene has unique properties and displays different results. To fully clarify the antibacterial mechanism of GrNs, detailed research is needed. To the best of our knowledge, such interactions of bacteria with GrNs synthesized onto various substrates (G and Ni) via different deposition methods (CVD and PECVD), and the evaluation according to the number of layers of graphene, have not been comparatively reported previously, and the findings may offer new viewpoints both for the better interpreting of the antibacterial activity of GrNs and for the better designing of graphene-based food-packing and biomedical device applications.

Author Contributions: Conceptualization, E.O.; methodology, E.O. and L.A.; validation, L.A. and B.A.; formal analysis, E.O., L.A. and B.A.; investigation, E.O.; resources, E.O.; writing—original draft preparation, E.O., F.O. and T.V.; writing—review and editing, E.O., F.O. and T.V.; visualization, E.O., F.O. and T.V.; supervision, F.O. and T.V. All authors have read and agreed to the published version of the manuscript.

Funding: This research was funded by Gazi University, grant number 18/2015–03.

Institutional Review Board Statement: Not applicable.

Informed Consent Statement: Not applicable.

Data Availability Statement: The data presented in this study are available on request from the corresponding author. The data are not publicly available due to restrictions privacy and ethical.

Acknowledgments: The authors would like to thank the Gazi University Electro-Optic Research Laboratory and Gazi University Molecular Biology Laboratory.

Conflicts of Interest: The authors declare no conflict of interest.

References

1. Yu, Q.; Wu, Z.; Chen, H. Dual-function antibacterial surfaces for biomedical applications. *Acta Biomater.* **2015**, *16*, 1–13. [CrossRef]
2. Aliamradni, V.; Abolmaali, S.S.; Borandeh, S. Antifungal and Antibacterial Properties of Graphene-based Nanomaterials: A Mini-review. *J. Nanostruct.* **2019**, *9*, 402–413.
3. Wei, C.; Lin, W.Y.; Zainal, Z.; Williams, N.E.; Zhu, K.; Kruzic, A.P.; Smith, R.L.; Rajeshwar, K. Bactericidal Activity of TiO2 Photocatalyst in Aqueous Media: Toward a Solar-Assisted Water Disinfection System. *Environ. Sci. Technol.* **1994**, *28*, 934–938. [CrossRef] [PubMed]
4. Kumar, A.; Vemula, P.K.; Ajayan, P.M.; John, G.C. Silver-nanoparticle-embedded antimicrobial paints based on vegetable oil. *Nat. Mater.* **2008**, *7*, 236–241. [CrossRef]
5. Schipper, M.L.; Nakayama-Ratchford, N.; Davis, C.R.; Kam, N.W.S.; Chu, P.; Liu, Z.; Sun, X.; Dai, H.; Gambhir, S.S. A pilot toxicology study of single-walled carbon nanotubes in a small sample of mice. *Nat. Nanotechnol.* **2008**, *3*, 216–221. [CrossRef] [PubMed]
6. Shen, H.; Zhang, L.; Liu, M.; Zhang, Z. Biomedical Applications of Graphene. *Theranostics* **2012**, *2*, 283–294. [CrossRef]
7. Zhang, Q.; Wu, Z.; Li, N.; Pu, Y.; Wang, B.; Zhang, T.; Tao, J. Advanced review of graphene-based nanomaterials in drug delivery systems: Synthesis, modification, toxicity and application. *Mater. Sci. Eng. C* **2017**, *77*, 1363–1375. [CrossRef]
8. Lin, J.; Chen, X.; Huang, P. Graphene-based nanomaterials for bioimaging. *Adv. Drug Deliv. Rev.* **2016**, *105*, 242–254. [CrossRef] [PubMed]
9. Goenka, S.; Sant, V.; Sant, S. Graphene-based nanomaterials for drug delivery and tissue engineering. *J. Control. Release* **2014**, *173*, 75–88. [CrossRef]
10. Tonelli, F.M.P.; Goulart, V.A.M.; Gomes, K.N.; Ladeira, M.S.; Santos, A.K.; Lorençon, E.; Ladeira, L.O.; Resende, R.R. Graphene-based nanomaterials: Biological and medical applications and toxicity. *Nanomedicine* **2015**, *10*, 2423–2450. [CrossRef]
11. Akhavan, O.; Ghaderi, E. Toxicity of Graphene and Graphene Oxide Nanowalls against Bacteria. *ACS Nano* **2010**, *4*, 5731–5736. [CrossRef]
12. Akhavan, O.; Ghaderi, E. Escherichia coli bacteria reduce graphene oxide to bactericidal graphene in a self-limiting manner. *Carbon* **2012**, *50*, 1853–1860. [CrossRef]
13. Al-Thani, R.F.; Patan, N.K.; Al-Maadeed, S. Graphene oxide as antimicrobial against two gram-positive and two gram-negative bacteria in addition to one fungus. *Online J. Biol. Sci.* **2014**, *14*, 230–239. [CrossRef]
14. Liu, S.; Zeng, T.H.; Hofmann, M.; Burcombe, E.; Wei, J.; Jiang, R.; Kong, J.; Chen, Y. Antibacterial Activity of Graphite, Graphite Oxide, Graphene Oxide, and Reduced Graphene Oxide: Membrane and Oxidative Stress. *ACS Nano* **2011**, *5*, 6971–6980. [CrossRef] [PubMed]
15. Pinto, A.M.; Gonçalves, I.; Magalhães, F. Graphene-based materials biocompatibility: A review. *Colloids Surf. B* **2013**, *111*, 188–202. [CrossRef]
16. Geim, A.K.; Novoselov, K.S. *Nanoscience and Technology: A Collection of Reviews from Nature Journals*; The Rise of Graphene; World Scientific: Singapore, 2010; pp. 11–19.
17. Jiang, H. Chemical Preparation of Graphene-Based Nanomaterials and Their Applications in Chemical and Biological Sensors. *Small* **2011**, *7*, 2413–2427. [CrossRef]
18. Xiao, F.; Li, Y.; Zan, X.; Liao, K.; Xu, R.; Duan, H. Growth of Metal-Metal Oxide Nanostructures on Freestanding Graphene Paper for Flexible Biosensors. *Adv. Funct. Mater.* **2012**, *22*, 2487–2494. [CrossRef]
19. Efil, E.; Kaymak, N.; Seven, E.; Orhan, E.O.; Bayram, O.; Ocak, S.B.; Tataroglu, A. Current–voltage analyses of Graphene-based structure onto Al_2O_3/p-Si using various methods. *Vacuum* **2020**, *181*, 109654. [CrossRef]
20. Kaymak, N.; Bayram, O.; Tataroğlu, A.; Ocak, S.B.; Orhan, E.O. Electrical properties of Graphene/Silicon structure with Al2O3 interlayer. *J. Mater. Sci. Mater. Electron.* **2020**, *31*, 9719–9725. [CrossRef]
21. Orhan, E.O.; Efil, E.; Bayram, O.; Kaymak, N.; Berberoğlu, H.; Candemir, O.; Pavlov, I.; Ocak, S.B. 3D-graphene-laser patterned p-type silicon Schottky diode. *Mater. Sci. Semicond. Process.* **2020**, *121*, 105454. [CrossRef]
22. Kaymak, N.; Orhan, E.O.; Bayram, O.; Ocak, S.B. Dielectric characteristics and electrical conductivity behavior of graphene/Al2O3/p-type silicon structure. *Mater. Chem. Phys.* **2020**, *258*, 123878. [CrossRef]

23. Li, J.; Wang, G.; Zhu, H.; Zhang, M.; Zheng, X.; Di, Z.; Liu, X.; Wang, X. Antibacterial activity of large-area monolayer graphene film manipulated by charge transfer. *Sci. Rep.* **2014**, *4*, 4359. [CrossRef]
24. Krishnamoorthy, K.; Veerapandian, M.; Zhang, L.-H.; Yun, K.; Kim, S.J. Antibacterial Efficiency of Graphene Nanosheets against Pathogenic Bacteria via Lipid Peroxidation. *J. Phys. Chem. C* **2012**, *116*, 17280–17287. [CrossRef]
25. Cao, G.; Yan, J.; Ning, X.; Zhang, Q.; Wu, Q.; Bi, L.; Zhang, Y.; Han, Y.; Guo, J. Antibacte-rial and antibiofilm properties of graphene and its derivatives. *Colloids Surf. B* **2021**, *200*, 111588. [CrossRef] [PubMed]
26. Dellieu, L.; Lawarée, E.; Reckinger, N.; Didembourg, C.; Letesson, J.-J.; Sarrazin, M.; Deparis, O.; Matroule, J.-Y.; Colomer, J.-F. Do CVD-grown graphene films have antibacterial activity on metallic substrates? *Carbon* **2015**, *84*, 310–316. [CrossRef]
27. Kumar, P.; Huo, P.; Zhang, R.; Liu, B. Antibacterial Properties of Graphene-Based Nanomaterials. *Nanomaterials* **2019**, *9*, 737. [CrossRef] [PubMed]
28. Avila-Alfaro, J.A.; Sánchez-Valdes, S.; Ramos-Devalle, L.F.; Ortega-Ortiz, H.; Méndez-Nonell, J.; Patiño-Soto, A.P.; Narro-Cespedes, R.I.; Perera-Mercado, Y.A.; Avalosbelmontes, F. Ultrasound Irradiation Coating of Silver Nanoparticle on ABS Sheet Surface. *J. Inorg. Organomet. Polym. Mater.* **2013**, *23*, 673–683. [CrossRef]
29. Karimi, L.; Yazdanshenas, M.E.; Khajavi, R.; Rashidi, A.; Mirjalili, M. Using graphene/TiO_2 nanocomposite as a new route for the preparation of electroconductive, self-cleaning, antibacterial, and antifungal cotton fabric without toxicity. *Cellulose* **2014**, *21*, 3813–3827. [CrossRef]
30. Díez-Pascual, A.M.; Díez-Vicente, A.L. Poly(propylene fumarate)/Polyethylene Glycol-Modified Graphene Oxide Nanocomposites for Tissue Engineering. *ACS Appl. Mater. Interfaces* **2016**, *8*, 17902–17914. [CrossRef]
31. Barbiroli, A.; Bonomi, F.; Capretti, G.; Iametti, S.; Manzoni, M.; Piergiovanni, L.; Rollini, M. Antimicrobial activity of lyso-zyme and lactoferrin incorporated in cellulose-based food packaging. *Food Control* **2012**, *26*, 387–392. [CrossRef]
32. Hu, W.; Peng, C.; Luo, W.; Lv, M.; Li, X.; Li, D.; Huang, Q.; Fan, C. Graphene-Based Antibacterial Paper. *ACS Nano* **2010**, *4*, 4317–4323. [CrossRef] [PubMed]
33. Rana, D.; Matsuura, T. Surface Modifications for Antifouling Membranes. *Chem. Rev.* **2010**, *110*, 2448–2471. [CrossRef] [PubMed]
34. Lok, C.-N.; Ho, .C.-M.; Chen, R.; He, Q.-Y.; Yu, W.-Y.; Sun, .H.; Tam, .P.K.-H.; Chiu, J.-F.; Che, C.M. Proteomic Analysis of the Mode of Antibacterial Action of Silver Nanoparticles. *J. Proteome Res.* **2006**, *5*, 916–924. [CrossRef] [PubMed]
35. Ahamed, M.; AlSalhi, M.; Siddiqui, M. Silver nanoparticle applications and human health. *Clin. Chim. Acta* **2010**, *411*, 1841–1848. [CrossRef] [PubMed]
36. Perreault, F.; Faria, A.F.; Nejati, S.; Elimelech, M. Antimicrobial Properties of Graphene Oxide Nanosheets: Why Size Matters. *ACS Nano* **2015**, *9*, 7226–7236. [CrossRef] [PubMed]
37. Ibarra-Alonso, M.; Sanchez-Valdes, S.; Ramírez-Vargas, E.; Fernandez-Tavizón, S.; Romero-Garcia, J.; Ledezma-Pérez, A.; De Valle, L.R.; Rodríguez-Fernández, O.; Espinoza-Martinez, A.; Martínez-Colunga, J.; et al. Preparation and characterization of Polyethylene/Clay/Silver nanocomposites using functionalized polyethylenes as an adhesion promoter. *J. Adhes. Sci. Technol.* **2015**, *29*, 1911–1923. [CrossRef]
38. Pham, V.T.; Truong, V.K.; Quinn, M.D.; Notley, S.M.; Guo, Y.; Baulin, V.A.; Kobaisi, M.A.; Crawford, R.J.; Ivanova, E.P.; Ivanova, E.P. Graphene induces formation of pores that kill spherical and rod-shaped bacteria. *ACS Nano* **2015**, *9*, 8458–8467. [CrossRef] [PubMed]
39. Navarro-Rosales, M.; Ávila-Orta, C.A.; Neira-Velázquez, M.G.; Ortega-Ortiz, H.; Hernández-Hernández, E.; Solís-Rosales, S.G.; Sánchez, B.L.E.; Morones, P.G.; Jiménez, R.; Sánchez-Valdes, S.; et al. Effect of Plasma Modification of Copper Nanoparticles on their Antibacterial Properties. *Plasma Process. Polym.* **2014**, *11*, 685–693. [CrossRef]
40. Bayram, O.; Igman, E.; Guney, H.; Demir, Z.; Yurtcan, M.T.; Cirak, C.; Hasar, U.C.; Simsek, O. Graphene/polyaniline nanocomposite as platinum-free counter electrode material for dye-sensitized solar cell: Its fabrication and photovoltaic performance. *J. Mater. Sci. Mater. Electron.* **2020**, *31*, 10288–10297. [CrossRef]
41. Igman, E.; Bayram, O.; Mavi, A.; Hasar, U.C.; Simsek, O. Photovoltaic performance of non-covalent functionalized single-layer graphene in dye-sensitized solar cells (DSSCs). *J. Mater. Sci.* **2020**, *56*, 4184–4196. [CrossRef]
42. Bayram, O. A study on 3D graphene synthesized directly on Glass/FTO substrates: Its Raman mapping and optical properties. *Ceram. Int.* **2019**, *45*, 16829–16835. [CrossRef]
43. Bayram, O.; Şimşek, O. Vertically oriented graphene nanosheets grown by plasma-enhanced chemical vapor deposition technique at low-temperature. *Ceram. Int.* **2019**, *45*, 13664–13670. [CrossRef]
44. Saeed, M.; Alshammari, Y.; Majeed, S.A.; Al-Nasrallah, E. Chemical Vapour Deposition of Graphene—Synthesis, Characterisation, and Applications: A Review. *Molecules* **2020**, *25*, 3856. [CrossRef] [PubMed]